2013

Magnetism and the magnetocaloric effect in PrMn1. 6Fe0. 4Ge2

W D. Hutchison
University of New South Wales

Jianli Wang
University of Wollongong, jianli@uow.edu.au

S J. Campbell
University of New South Wales

Magnetism and the magnetocaloric effect in PrMn1. 6Fe0. 4Ge2

Abstract

The magnetic and magnetocaloric properties of PrMn1.6Fe0.4Ge2around the ferromagnetic transitions T C inter ~ 230 K and T C Pr ~ 30 K have been investigated by magnetisation, 57Fe Mössbauer spectroscopy and electron paramagnetic resonance (EPR) measurements over the temperature range 5–300 K. The broad peaks in magnetic entropy around TC inter (intralayer antiferromagnetism of the Mn sublattice to canted ferromagnetism) and TC Pr (onset of ferromagnetic order of Pr sublattice in addition to ferromagnetically ordered Mn sublattice) are typical of second order transitions with maximum entropy values of -ΔS M ~ 2.0 J/kg K and -ΔS M ~ 2.2 J/kg K respectively for ΔB = 0–6 T. The EPR signal around T = 48 K of g value g ~ 0.8 is consistent with paramagnetic free ion Pr3 + . Below TC Pr ~ 30 K the g value increases steadily to g ~ 2.5 at 8 K as saturation of the Pr3 + ion is approached. The EPR measurements indicate additional effects in this system below T ~ 20 K with the appearance of EPR signals of low g value g ~ 0.6.

Keywords

effect, prmn1, 6fe0, magnetocaloric, magnetism, 4ge2

Disciplines

Engineering | Physical Sciences and Mathematics

Publication Details

Hutchison, W. D., Wang, J. L. & Campbell, S. J. (2013). Magnetism and the magnetocaloric effect in PrMn1. 6Fe0. 4Ge2. Hyperfine Interactions, 221 (1-3), 35-43.

Magnetism and the Magnetocaloric Effect in $PrMn_{1.6}Fe_{0.4}Ge_2$

W. D. Hutchison[1], J.L. Wang[1,2,3] and S.J. Campbell[1]

[1]School of Physical, Environmental and Mathematical Sciences,

The University of New South Wales, Canberra, ACT 2600 Australia

[2]Institute for Superconductivity and Electronic Materials, University of Wollongong,

Wollongong, NSW 2522 Australia

[3]Bragg Institute, ANSTO, Menai, NSW 2234 Australia

Abstract: The magnetic and magnetocaloric properties of $PrMn_{1.6}Fe_{0.4}Ge_2$ around the ferromagnetic transitions T_C^{inter} ~ 230 K and T_C^{Pr} ~ 30 K have been investigated by magnetisation, ^{57}Fe Mössbauer spectroscopy and electron paramagnetic resonance (EPR) measurements over the temperature range 5-300 K. The broad peaks in magnetic entropy around T_C^{inter} (intralayer antiferromagnetism of the Mn sublattice to canted ferromagnetism) and T_C^{Pr} (onset of ferromagnetic order of Pr sublattice in addition to ferromagnetically ordered Mn sublattice) are typical of second order transitions with maximum entropy values of $-\Delta S_M$ ~ 2.0 J/kg K and $-\Delta S_M$ ~ 2.2 J/kg K respectively for ΔB = 0-6 T. The EPR signal around T = 48 K of g value g ~ 0.8 is consistent with paramagnetic free ion Pr^{3+}. Below T_C^{Pr} ~ 30 K the g value increases steadily to g ~ 2.5 at 8 K as saturation of the Pr^{3+} ion is approached. The EPR measurements indicate additional effects in this system below T ~ 20 K with the appearance of EPR signals of low g value g ~ 0.6.

Key words: Magnetisation, ^{57}Fe Mössbauer Spectroscopy, EPR, Magnetic Entropy, $PrMn_{1.6}Fe_{0.4}Ge_2$

Corresponding Author: Email: Stewart.Campbell@adfa.edu.au

Tel: +61 2 6268 8767; Fax: +61 2 6268 8786

1. Introduction

In addition to the continuing intrinsic interest in understanding the myriad of structural and physical properties exhibited by RMn_2X_2–based compounds (X=Si, Ge) [e.g. 1-3], such rare earth (R)-transition metal intermetallic compounds have attracted additional attention due to their magnetocaloric behaviour at selected magnetic transitions [e.g. 4-6]. For example, $NdMn_2Ge_{0.4}Si_{1.6}$ has recently been shown to exhibit a giant magnetocaloric effect (MCE) associated with the field-induced first order magnetic transition (FOMT) from antiferromagnetism to ferromagnetism around T_C ~ 36 K [6]. Magnetic materials around these temperatures are relevant to cooling aspects related, for example, to magnetic refrigeration for hydrogen liquefaction [7].

The structural and magnetic behaviours of the $PrMn_{2-x}Fe_xGe_2$ series of compounds have been investigated and the magnetic phase diagram determined [e.g. 8, 9]. Of particular interest are Mn-rich compounds around x ~ 0.4 for which ferromagnetic transitions are obtained around T_C^{inter} ~ 230 K and T_C^{Pr} ~ 30 K [9]. The transition at T_C^{inter} marks the change in magnetic ordering of the Mn sub-lattice from in-plane intralayer antiferromagnetism (AFl) to canted ferromagnetism (Fmc) where the ferromagnetic component is aligned along the c-axis in addition to the persistent intralayer antiferromagnetism [8, 9]. Below T_C^{Pr} the Pr sublattice orders ferromagnetically with moments along the c-axis, resulting in the combined magnetic region (Fmc+F(Pr)). The magnetic structures are described using the notation of Venturini *et al.* [10] with the $PrMn_{2-x}Fe_xGe_2$ structures depicted in [8]. Here we present the results of an investigation of the ferromagnetic transitions in $PrMn_{1.6}Fe_{0.4}Ge_2$ and their magnetic entropy behaviour by a combination of magnetisation and ^{57}Fe Mössbauer spectroscopy measurements over the temperature range 5-300 K. Electron paramagnetic resonance (EPR), focusing on the Pr^{3+} 4f magnetic moment, has been applied for the first time to provide insight to ordering of the Pr sublattice below T_C^{Pr}~30 K and its interaction with the canted ferromagnetic Mn sublattice.

2. Experimental

The $PrMn_{1.6}Fe_{0.4}Ge_2$ compound was prepared by argon arc melting appropriate amounts of high purity elements on a water-cooled Cu hearth. As described previously [9, 11], ~2-3% excess Mn was used to compensate for loss during melting and the samples were doped with ~3.5 at.% enriched ^{57}Fe to enhance the sensitivity of the ^{57}Fe Mössbauer experiments. The sample was re-melted five times to ensure good homogeneity and annealed at 900°C for one week in an evacuated quartz tube. X-ray diffraction (CuK_α) confirmed that the sample exhibited the body-centred tetragonal structure of space group I4/mmm as expected [e.g. 8, 9] with no discernible impurity phases; this indicates that impurities, if present, occur at less than ~2%. Rietveld refinement of the pattern resulted in cell parameters a = 4.100(1) Å and c = 10.869(1) Å. The magnetic measurements were carried out using a Physical Property Measurement System over the temperature range 5-300 K and at magnetic fields in the range 0-6 T. ^{57}Fe Mössbauer spectra were obtained between 4.5 K and 300 K using a standard constant-acceleration spectrometer and a $^{57}CoRh$ source and the spectrometer calibrated at room temperature with an α-iron foil. The EPR measurements were carried out using a Bruker spectrometer fitted with a standard x band cavity and a helium flow cryostat over the temperature range 8-50 K.

3. Results and Discussion

3.1 Magnetisation; Magnetocaloric Effect: The temperature dependences of the magnetisation of $PrMn_{1.6}Fe_{0.4}Ge_2$ as measured in a field of B=0.01 T on warming and cooling, after initial cooling in zero field, are shown in Fig 1. The warming and cooling directions are marked by arrows with the initial cooling curve omitted. The differences in magnetisation between the cooling and warming curves reflect magneto-history effects [12] in this compound and are ascribed to the presence of narrow domain walls [13]. As expected on the basis of previous studies [9], the present sample was found to exhibit magnetic transitions around T_C^{Pr} ~ 30 K and T_C^{inter} ~ 230 K (the higher temperature transition from

paramagnetism to antiferromagnetism at T_N^{intra} ~ 370 K was not explored in the present investigation).

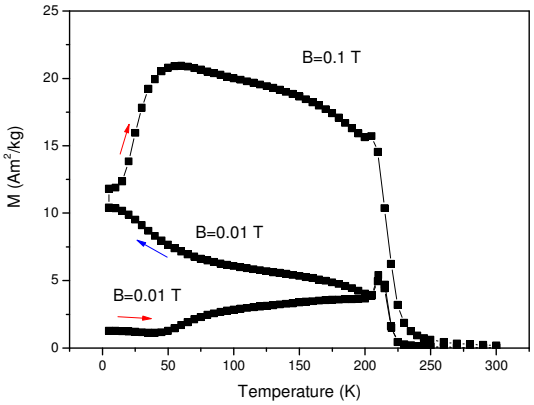

Fig. 1 The temperature dependence of the magnetisation of $PrMn_{1.6}Fe_{0.4}Ge_2$ as measured in a field of B = 0.01 T on warming and cooling (as marked by arrows) after first cooling in zero field (the initial cooling curve is omitted). The pronounced differences in these curves reflect magneto-history effects ascribed to the presence of narrow domain walls.

The variable temperature magnetisation curves (M versus B) and the related Arrott plots (M^2 versus B/M) for $PrMn_{1.6}Fe_{0.4}Ge_2$ over the range T=5-250 K are shown in Figs. 2(a) and 2(b) respectively with the ferromagnetic natures of the phases below T_C^{inter} ~ 230 K and T_C^{Pr} ~ 30 K evident. The positive slope of the Arrott plots around T_C^{Pr} and T_C^{inter} (see for example, analysis of re-entrant ferromagnet $PrMn_2Ge_{0.8}Si_{1.2}$ [11]) combined with the absence of field hysteresis around either T_C^{Pr} or T_C^{inter}, demonstrates that both magnetic phase transitions are second order.

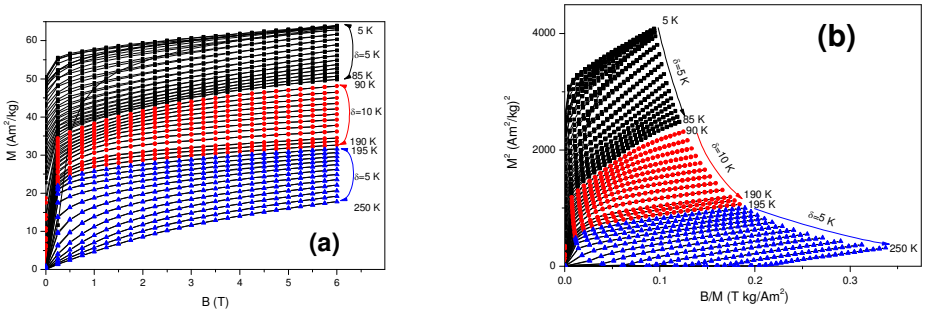

Fig. 2(a) Magnetisation versus field curves (B=0-6 T) for $PrMn_{1.6}Fe_{0.4}Ge_2$ over the temperature regions around T_C^{inter} ~ 230 K and T_C^{Pr} ~ 30 K.

(b) Arrott plots of M^2 versus B/M for $PrMn_{1.6}Fe_{0.4}Ge_2$.

The isothermal entropy change $-\Delta S_M$ corresponding to a magnetic field change ΔB from B = 0 to value B, has been derived from the magnetisation data using the Maxwell relation:

$$\Delta S_M(T,B) = \mu_0 \int_0^B \left(\frac{\partial M}{\partial T}\right)_B dB \,. \qquad (1)$$

The changes in magnetic entropy $-\Delta S_M$ as functions of temperature and external field are shown in Fig. 3. The curves of $-\Delta S_M$ exhibit a broad peak around T_C^{Pr} and T_C^{inter} - behaviour typical of a second order phase transition - with maximum values (for ΔB = 0-6 T) around T_C^{Pr} and T_C^{inter} of $-\Delta S_M \sim 2.0$ J/kg K and $-\Delta S_M \sim$ 2.2 J/kg K respectively. The insert to Fig. 3 shows a graph of maximum entropy change $-\Delta S_M^{max}$ plotted as a function of $(B/T_C)^{2/3}$ for data in the region around T_C^{Pr} and T_C^{inter}. Mean field theory [see e.g. 11] predicts that $-\Delta S_M$ is proportional to $(B/T_C)^{2/3}$ at second order phase transitions with the well behaved linear fits in insert to Fig. 3 demonstrating that the relationship $-\Delta S_M^{max} \propto (B/T_C)^{2/3}$ is applicable around T_C^{Pr} and T_C^{inter} for $PrMn_{1.6}Fe_{0.4}Ge_2$, thus confirming the second order nature of these ferromagnetic transitions.

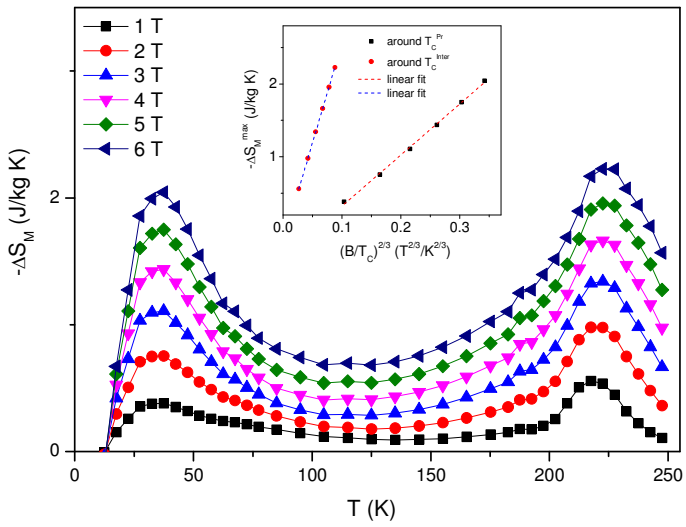

Fig. 3 Temperature dependence of the isothermal magnetic entropy change $-\Delta S_M(T, B)$ for $PrMn_{1.6}Fe_{0.4}Ge_2$ as measured in magnetic fields up to 6 T. The insert shows graphs of $-\Delta S_M^{max}$ versus $(B/T_C)^{2/3}$ for $PrMn_{1.6}Fe_{0.4}Ge_2$ around $T_C^{Pr} \sim 30$ K and $T_C^{inter} \sim 230$ K. The dashed lines represent linear fits to the data as discussed in the text.

3.2 Mössbauer Spectroscopy: The Mössbauer spectra at T = 235 K and T =100 K (Fig. 4(a)) reveal magnetic hyperfine splitting as expected for $PrMn_{1.6}Fe_{0.4}Ge_2$ in the magnetically ordered AFl antiferromagnetic and Fmc canted ferromagnetic phases respectively [9, 14]. The Mössbauer spectra were fitted using a binomial distribution model for the iron atoms in which four sub-sextets (dashed lines) represent Fe atoms with zero, one, two and three (or more) nearest neighbours Fe atoms (the fractional areas of the sub-spectra are 0.410, 0.410, 0.154 and 0.027, respectively; see [14] for details). At 5 K, the individual hyperfine fields for these four sub-sextets are derived to be 10.6 T, 9.1 T, 5.8 T and 4.1 T respectively with the average hyperfine field B_{hf}(average) = 9.1 T. Given that Fe atoms do not carry a magnetic moment in RFe_2X_2 or in ^{57}Fe doped RT_2X_2 compounds (T=transition metal) [15], the sub-spectrum with the largest B_{hf} is attributed to Fe atoms having the largest Mn coordination (i.e. zero Fe nn) with the smallest B_{hf} attributed to Fe atoms having the largest Fe coordination (three or more nn).

As noted previously and shown in Fig 4(b), [14], the discontinuities in the magnetisation versus temperatures curves around T_C^{Pr} and T_C^{inter} evident in Fig. 1, are reflected by the changing trends in the temperature dependence of the average hyperfine field. The observed hyperfine fields result from contributions to the exchange interactions present in the Pr and Mn sublattices and correspondingly reflect the magnetic order in the Pr and Mn sublattices leading to the changes in behaviour of the B_{hf} values around the ordering temperatures. It is also of interest to note the discontinuity in the quadrupole shift ε values at the magnetic phase transition temperatures which may be due to a possible distortion of the unit cell and/or the variation in the magnetic ordering of the Mn moment [14]. The dashed line through the isomer shift data represents a fit of the second-order Doppler shift in terms of the Debye model for the phonon spectrum leading to the Debye temperature for $PrMn_{1.6}Fe_{0.4}Ge_2$ of θ_D = 350 ± 20 K (see [9] for details). The Debye temperatures for compounds in the $PrMn_{2-x}Fe_xGe_2$ series increase with increasing Fe content consistent with the difference in Debye temperatures between Mn of θ_D^{Mn} = 400 K and Fe of θ_D^{Fe} = 460 K [9].

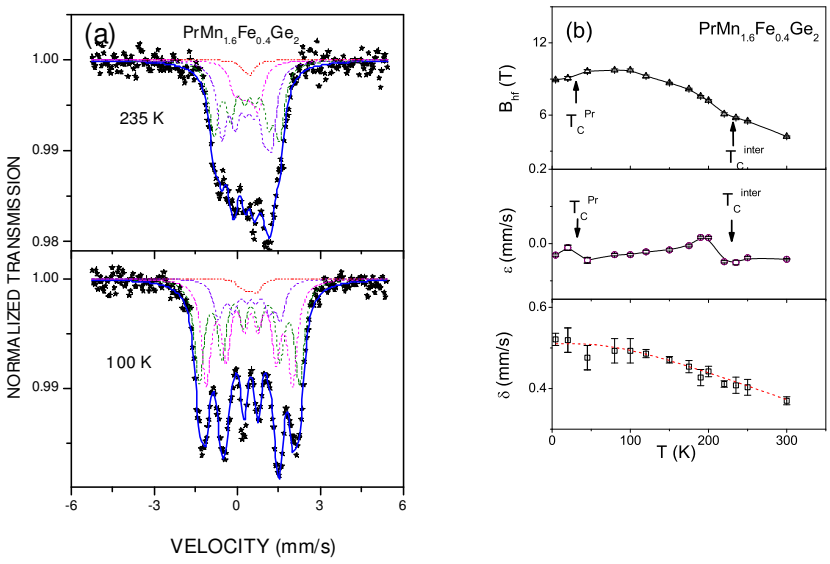

Figure 4(a) Mössbauer spectra of $PrMn_{1.6}Fe_{0.4}Ge_2$ at T = 235 K and T = 100 K in the antiferromagnetic and canted ferromagnetic phases respectively. The fits and sub-spectra are described in the text.

(b) The temperature dependences of the average values of magnetic hyperfine field B_{hf}, quadrupole shift ε and isomer shift δ for $PrMn_{1.6}Fe_{0.4}Ge_2$ [14]. The full lines are guides to the eye through the B_{hf} and ε data with the dashed line through the δ data representing a fit using the Debye model leading to $\theta_D = 350 \pm 20$ K.

3.3 Electron Paramagnetic Resonance: As noted above, interest focuses on the Pr^{3+} 4f magnetic moment of $PrMn_{1.6}Fe_{0.4}Ge_2$ and its EPR response at the onset of ordering of the Pr sublattice around $T_C^{Pr} \sim 30$ K. A selection of the electron paramagnetic resonance spectra which were collected for $PrMn_{1.6}Fe_{0.4}Ge_2$ over the temperature range 8-48 K is shown in Fig. 5. In addition to the predominant EPR signal present at all temperatures, as discussed below, significant second and third lines occur in the EPR spectra at temperatures below T ~ 20 K. The EPR spectra were fitted well with differential Gaussian line shapes, allowing for up to three lines and a sloping baseline. The g values, corresponding to centres of the fitted lines, are shown as a function of temperature in Fig. 6. For the purpose of this preliminary analysis additional second order structure that becomes just apparent at the very lowest temperatures and may reflect impurity phase/s or crystal asymmetry, is ignored.

Several important features can be noted from Figures 5 and 6. At temperatures well above T_C^{Pr}, for example T = 48 K, a single line of value g ~ 0.85 is obtained. This behaviour is consistent with the paramagnetic free ion Pr^{3+} Landé value of g = 0.8 and we therefore conclude that the signals of Fig. 5 are due to the EPR response of the Pr ion. The g value of this principle line (line 1) increases with decrease in temperature and exhibits a rapid increase below ~ 20 K to g ~ 2.5 at 8 K; this behaviour correlates well with the onset of Pr ordering below T_C^{Pr} ~ 30 K. Also evident in Fig. 5 is the appearance below ~ 20 K of a second line at g ~ 0.60 which increases in intensity as the temperature decreases further and eventually, below T ~ 10 K, resolves into two lines, with this third line having an approximate g value of ~ 0.57. This behaviour could be associated with the transition from the Fmc ordered Mn sublattice state above T_C^{Pr} ~ 30 K to the region below T_C^{Pr} where the ordered Mn and Pr sublattices coexist. However, the appearance of these additional lines below T_C^{Pr} is most likely due to developing population asymmetry in low lying crystal field levels or indeed, to a slight structural change associated with the magnetic phase transition at T_C^{Pr}. It is also noted that the boundary between the canted ferromagnetic Fmc and the conical ferromagnetic Fmi phases in $PrMn_{2-x}Fe_xGe_2$ occurs around these temperatures for Fe concentration x ~ 0.4 (see Fig. 12 of [9]), with the conical Fmi structure having been determined for $PrMn_2Ge_2$ by Welter *et al.* [16]. It is possible that the additional complexity in the EPR spectra below ~ 20 K may be an indicator of the phase transition between the ordered Fmc and Fmi Mn sublattices that occurs in the region of co-existing order of the Pr sublattice. While further analyses and investigation of these EPR data are continuing [17], it is clear that electron paramagnetic resonance provides a further sensitive probe to the investigation of these fascinating series of RT_2X_2 compounds.

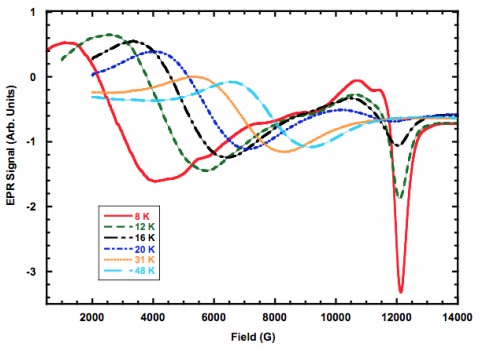

Figure 5: Selected EPR spectra for $PrMn_{1.6}Fe_{0.4}Ge_2$ recorded in the temperature range 8 K to 48 K.

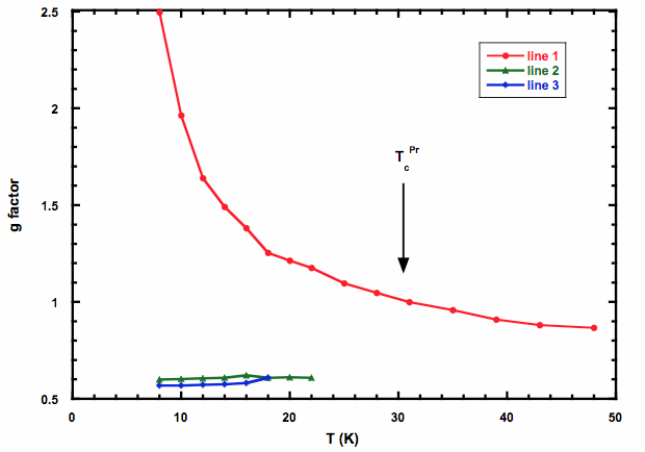

Figure 6: Pr^{3+} g factors determined by fitting differential Gaussian line shapes to the EPR spectra recorded at various temperatures in the range 8 to 48 K. The solid lines are guides for the eye. The EPR signals (*cf.* Fig. 5) are numbered as lines 1, 2, 3 in descending g value.

4. Conclusions

The ferromagnetic transitions T_C^{inter} ~ 230 K and T_C^{Pr} ~ 30 K of $PrMn_2Ge_{0.8}Si_{1.2}$ are found to be continuous second order transitions with broad peaks in magnetic entropy $-\Delta S_M$ as functions of temperature and external field. The maximum entropy values around T_C^{inter} and T_C^{Pr} are $-\Delta S_M$ ~ 2.2 J/kg K and $-\Delta S_M$ ~ 2.0 J/kg K (ΔB = 0-6 T) respectively. The magnetic transitions around T_C^{inter} and T_C^{Pr} are also marked by changes in the magnetic hyperfine field and quadrupole shift parameters with the isomer shift leading to the Debye temperature θ_D = 350 ± 20 K for $PrMn_{1.6}Fe_{0.4}Ge_2$. Electron paramagnetic resonance spectra below T ~ 50 K reveal a predominant signal due to the Pr^{3+} ion with the value g = 0.85 in the paramagnetic region above T_C^{Pr} ~ 30 K found to increase to g ~ 2.5 at 8 K as the 4f magnetic moment of $PrMn_{1.6}Fe_{0.4}Ge_2$ tends towards saturation.

Acknowledgements

This work is supported by a grant from the Australian Research Council (DP110102386) and a joint agreement between ANSTO and the University of Wollongong. The EPR spectrometer at the Australian National University was in part funded by a joint ARC LIEF grant (LE100100177) and we thank Drs R. Pace and P. Smith for assistance.

References

[1] G. Venturini, R Welter, J E Ressouche, B. Malaman, J. Magn. Magn. Mater. **150**, 197 (1995)

[2] M. Hofmann, S.J. Campbell, A.V.J. Edge, Phys. Rev. B **69**, 174432 (2004)

[3] I Dincer, Y Elerman, A Elmali, H Ehrenberg, G André, J. Magn. Magn. Mater. **313,** 342 (2007)

[4] S. Kervan, A. Kilic and A. Gencer, J. Phys.: Condens. Matter **16**, 4955 (2004)

[5] K. Sengupta, P.L. Paulose, E.V. Sampathkumaran, T. Doert, and J.P.F. Jemetio, Phys. Rev. B **72,** 184424 (2005).

[6] J.L. Wang, S.J. Campbell, J.M. Cadogan, A.J. Studer, R. Zeng and S.X. Dou, Appl. Phys. Lett. **98**, 232509 (2011)

[7] K Matsumoto, T Kondo, S Yoshioka, K Kamiya and T Numazawa, J. Phys Conf Series **150**, 012028 (2009)

[8] I. Dincer, A. Elmali, Y. Elerman, H. Ehrenberg, H. Fuess and G. Andre, J. Alloy. Comp. **416**, 22 (2006)

[9] J.L. Wang, S.J. Campbell, A J Studer, M Avdeev, M Hofmann, M Hoelzel and S X Dou, J. Applied Physics **104**, 103911 (2008)

[10] G. Venturini, R. Welter, E. Ressouche and B. Malaman, J. Magn. Magn. Mater. **150**, 197 (1995)

[11] J. L. Wang, S. J. Campbell, R. Zeng, C. K. Poh, S. X. Dou, and S. J. Kennedy, J. Appl. Phys. **105**, 07A909 (2009)

[12] J. L. Wang, S. J. Campbell, O. Tegus, C. Marquina and M. R. Ibarra, Physical Review B **75**, 174423 (2007)

[13] J. L. Wang, C. C. Tang, G. H. Wu, Q. L. Liu, N. Tang, W. Q. Wang, W. H. Wang, F. M. Yang, J. K. Liang, F. R. de Boer, and K. H. J. Buschow, Solid State Commun. **121**, 615 (2002); J. L.Wang, C. Marquina, M. R. Ibarra, and G. H. Wu, Phys. Rev. B **73**, 094436 (2006).

[14] J.L. Wang, S.J. Campbell, J.M. Cadogan, O. Tegus, A.J. Studer and M. Hofmann, J. Phys.: Condens. Matter **18**, 189–204 (2006)

[15] Matúš Mihalik, Jana Vejpravová, Ján Rusz, Martin Diviš, Pavel Svoboda, and Vladimír Sechovský, Phys. Rev. B **70**, 134405 (2004)

[16] R. Welter, G. Venturini, E. Ressouche, and B. Malaman, J. Alloys Compd. **218**, 204 (1995)

[17] W. D. Hutchison, J. L. Wang and S. J. Campbell, (in preparation, 2012)